



Equilibrium and Kinetics Analysis on Vat Yellow 4 Uptake from Aqueous Environment by Modified Rubber Seed Shells: Nonlinear modelling

Chinenye Adaobi Igwegbe^{1*}, Okechukwu Dominic Onukwuli¹,
Kenechukwu Keluo Onyechi², Shahin Ahmadi³

¹Department of Chemical Engineering, Nnamdi Azikiwe University, Awka, Nigeria.

²Department of Pharmaceutics and Pharmaceutical Technology, Nnamdi Azikiwe University, Awka, Nigeria.

³Department of Environmental Health, School of Public Health, Zabol University of Medical Sciences, Zabol, Iran.

Received 07 April 2020,
Revised 26 July 2020,
Accepted 27 July 2020

Keywords

- ✓ Vat yellow
- ✓ Adsorption
- ✓ Activation energy
- ✓ Wastewater treatment
- ✓ Error functions

ca.igwegbe@unizik.edu.ng
Phone: +2348036805440;
ORCID: 0000-0002-5766-7047

Abstract

Rubber seed shells carbon (RSSC) was harnessed for the elimination of vat yellow 4 (VY4) from its liquid solution and its properties analysed. The process was optimised using the one-factor-at-a-time technique. The impact of RSSC dosage, pH, interaction time, temperature and VY4 concentration on VY4 adsorption onto RSSC was inspected. The error functions and coefficient of regression (R^2) were exercised as measures to decide the kinetic and isotherm models that best represents the results. High percentage of fixed carbon (82.54 %) and surface area (999 m^2/g) were observed on the RSSC. The SEM analysis revealed the high porosity of the RSSC. The XRF analysis indicated the presence of minerals ($K_2O = 8.2\%$, $Fe_2O_3 = 29.9\%$, $SiO_2 = 21\%$, and $CaO = 16.9\%$) which will favour the process of ion adsorption. Optimal conditions of interaction time: 90 min, temperature: 303 K, pH: 2, and RSSC dose: 1.0 g led to 84.34 % elimination with monolayer adsorption capacity (q_m) of 27.55 mg/g. The investigational results was best defined by the pseudo-first-order model; the Freundlich isotherm equation (with $R^2 = 0.9999$, RMSE = 0.033, $\chi^2 = 0.0443$) gave the best explanation for the results. The process was favourable since the separation factor ($R_L = 0.011$) lies within 0 and 1. The activation energy (94.7197 > 40 kJ/mol) and the mean sorption energy (0.0844 < 8 kJ/mol) suggest that the process could be chemically ordered. The process was spontaneous and endothermic in nature.

1. Introduction

The release of coloured wastewaters are threatening to the ecosystem and has caused a lot of concern. Dyes have been extensively excreted in the wastewater from different industries, particularly from textile, paper, rubber, plastic, leather, cosmetic, food, and drug industries which use dyes to colour their products [1]. Dyes are chemicals, which on binding with a material will give colour to them [2]. There are more than 10, 000 types of dyes commercially available, with over 7 - 105 tonnes of dyestuff produced annually, which can be classified according to their structure as anionic and cationic [3, 4]. Generally, the dyes that are used in the textile industry are basic dyes, acid dyes, reactive dyes, direct dyes, azo dyes, mordant dyes, vat dyes, disperse dyes and sulphur dyes [5].

Vat yellow 4 is a synthetic anthraquinone vat dye [6], which is applied in the dyeing of cotton, rayon, and wool by textile industries [7, 8]. They exhibit good fastness to light, acid, alkali, and solvents.

Vat dyes are carcinogenic [9] and toxic in nature. Dyes impede the transmission of light and thereby disturb the processes of biological metabolism when present in the aquatic environment [10]. Many dyes may cause allergic dermatitis, skin irritation, dysfunction of kidney, liver, brain, reproductive, and central nervous system. Besides, some are suspected carcinogens and mutagens [11]. Even a very low concentration of dye can make water unacceptable for various purposes [12]. Therefore, it is very important to treat effluents containing these dyes before discharge to the environment.

Many treatment methods have been adopted to remove dyes from wastewater including coagulation-flocculation [13, 14], electrocoagulation [15-17], adsorption [18-22], and advanced oxidation processes [23-25]. But the adsorption process is the most widely used method for the removal of colours and other pollutants [8, 26, 27]. Adsorption is a surface phenomenon that results from binding forces between atoms, molecules, and ions of adsorbate and the surface of the adsorbent. Adsorption may be classified as physisorption (due to Van der Waals forces and is reversible) and chemisorption (due to covalent or ionic bond) [28]. Factors that influence the rate of adsorption include the surface area of the adsorbent, the particle size of adsorbent, contact time, the solubility of solute (adsorbate) in liquid (wastewater), the affinity of the solute for the adsorbent, degree of ionization of the adsorbate molecule and pH of the adsorbate solution [29].

Different adsorbents have been used successfully for the adsorptive removal of vat dyes such as *Mucuna pruriens* seed shells [6], saw dust [10], MgO nanoparticles [30], waste ash [31] and rice husk [32]. Activated carbon, the most important commercial adsorbent, is a carbonaceous material with a large surface area and high porosity [33]. The large surface area results in a high capacity for adsorbing chemicals from gases and liquids [34]. The use of activated carbon has been highlighted as an effective technique for dye removal due to its unique molecular structure, high porosity, and an extensive surface area which makes them effective adsorbents for several toxic materials in wastewater treatment [35]. Adsorbents obtained from agricultural wastes are superior to other adsorbents because they are less expensive and readily available and can be used without or with a minimum of processing which in turn reduces the cost of production and energy associated with thermal treatment [36]. Agricultural wastes are lignocellulosic materials that consist of three main structural components which are lignin, cellulose, and hemicelluloses. Lignocellulosic materials constitute the more commonly used precursor and account for around 45 % of the total raw materials used for the manufacture of activated carbon [29]. Agricultural wastes are renewable, available in large amounts, and less expensive as compared to other materials used as adsorbents. The production of activated carbon from agricultural by-products has potential economic and environmental impacts. It converts unwanted, low – value agricultural waste to useful, high-value adsorbents.

Hevea brasiliensis (rubber) belongs to the family Spurge or Euphorbiaceae. The Hevea tree produces significant quantities of milk-like sap called latex, which is an emulsion of hydrocarbons in water. It is a material of industrial significance [37]. Rubber seed oil is extracted from the rubber seed. The rubber seed shell (RSS) is used as biofuel or manure or is discarded and allowed to rot [37]. Studies on the use of rubber seed shells or coat (RSS) has been reported for the sorption of different pollutants such as phenol [38], iron (111) ions [39], methylene blue [37], malachite green [40], congo red [41] and Rhodamin B [42]. To the best of our knowledge, the study of VY4 removal by rubber seed shells which has been used successfully as a good adsorbent has not been reported in the literature.

This study aimed to investigate the use of activated rubber seed shell carbon (RSSC) for the removal of VY4 dye from its aqueous solutions by adsorption technique. The effects of various parameters such as interaction time, initial pH, RSSC dose, temperature, and VY4 concentration were examined in the batch experiments and their optimal conditions determined. Also, the best adsorption

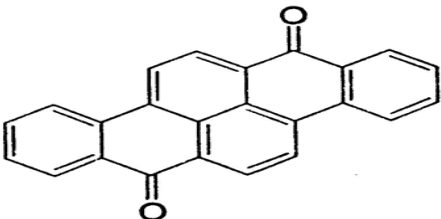
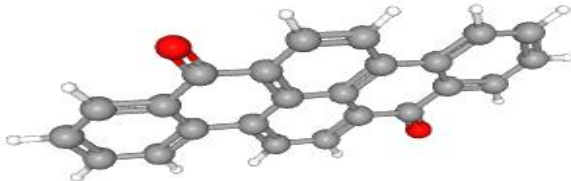
isotherm and kinetic models that best correlate the adsorption data were established using the nonlinear modelling technique. The activation energy and the parameters of thermodynamics of the VY4 adsorption on RSSC were also studied.

2. Experimental Material and Methods

2.1 Materials

Vat yellow, VY4 (other names: Golden Yellow GK, Dibenzochrysenedione, Dibenzpyrenequinone, Tyrian Yellow I-GOK, Dibenzo[b,def]chrysene-7,14-dione, 3,4:8,9-dibenzopyrene-5,10-dione) with percentage purity: 99.99% was purchased from a Nigerian chemicals market. The characteristics of the VY4 dye are presented in Table 1. Double-distilled water was used to prepare all solutions. The chemicals were of analytical grade and were used as-purchased without purification.

Table 1. Properties of VY4 dye.

C.I. name	Vat Yellow 4
Color index number	59100
Type of dye	Vat dye
Molecular weight, M_w (g/mol)	332.35
Maximum wavelength, λ_{max} (nm)	419
Molecular formula	$C_{24}H_{12}O_2$
Chemical structure	3D structure
	

2.2 Preparation of the adsorbent

Rubber seed shells (RSS) were collected from the Rubber Research Institute of Nigeria, Iyanomon, Benin city, Edo State, Nigeria, and washed thoroughly with deionized water to remove dirt and dried at 105°C for 24 h. It was ground, sieved to the desired particle size of 1-2 mm, and stored in a container. Before carbonization, the raw material can be impregnated with certain chemicals. It is believed that the carbonization/ activation step proceeds simultaneously with the chemical activation [29]. 100 g of the dried sample was soaked in 60 % phosphoric acid (H_3PO_4) in the weight ratio of 1:1 at room temperature for 24 h and carbonized under nitrogen (N_2) gas flow in a muffle furnace at 300°C for 3 h. The carbonized sample was cooled and washed with deionized water until a pH of 7 was reached. Finally, the sample was ground and sieved to different particle sizes and stored in airtight containers before use.

2.3. Characterisation of the adsorbent

The scanning electron microscopy (SEM) (Carl Zeis Analytical SEM Series.MA 10.EVO-10-09-49) was used to determine the surface structure of the RSSC. The functional groups present in the activated carbon (RSSC) responsible for the adsorption of VY4 were determined using the Fourier transform infrared (FTIR) (Shimadzu S8400 spectrophotometer), with the sample prepared by the conventional KBr disc method. The physicochemical properties of the RSSC were determined according to the method described by Nwabanne and Igbokwe [43]. Its chemical composition was also determined using the X-ray fluorescence (XRF), Philips PW 2400 XRF spectrometer.

2.4 Batch adsorption studies

A stock solution of VY4 was prepared by dissolving an appropriate mass of VY4 in double-distilled water where other concentrations were obtained by dilution. The influence of process variables including pH, mass of RSSC, solution temperature, initial VY4 concentration, and interaction time on the adsorption of VY4 on RSSC was investigated. 0.1 g VY4 was dissolved in 1000 mL of distilled water to get a dye solution of 100 mg/L. Batch adsorption experiments were executed by adding 100 mL stock solution of dye in 250 mL Erlenmeyer flask which was treated with a known mass of RSSC. The pH of the solution was adjusted using 0.1 M NaOH or HCl. The pH of the solution was determined using the potable pH meter. The content was shaken at 120 rpm using a stirrer at a specific temperature for the desired time of interaction. After the desired time of treatment, the solution was centrifuged and filtered. The concentration of the residue was determined using a UV-visible spectrophotometer (Model UV 752) at maximum absorbance, λ_{max} of 419 nm [6]. A calibration plot was made for VY4 to obtain a relation between its absorbance with its concentration. The percentage of VY4 removed, $R(\%)$ and the amount of VY4 adsorbed on RSSC, q_e (mg/g) was determined as follows [44, 45]:

$$R(\%) = \frac{C_0 - C_f}{C_0} \times 100 \quad (1)$$

$$q_e = \frac{(C_0 - C_e)V}{M} \quad (2)$$

where q_e is the equilibrium adsorption capacity (mg/g), C_0 is the initial concentration of VY4 in the solution (mg/L), C_e is the final or equilibrium concentration of VY4 in the solution (mg/L), V is the volume of the VY4 solution (L) treated, and W is the mass of RSSC used (g).

3. Results and discussion

3.1 Calibration curve for Vat Yellow 4

Figure 1 shows the vat yellow 4 (VY4) calibration curve in which the concentration of VY4 (in mg/L) can be evaluated if the absorbance of a solution containing VY4 is measured using the UV-visible spectrophotometer at λ_{max} of 419 nm.

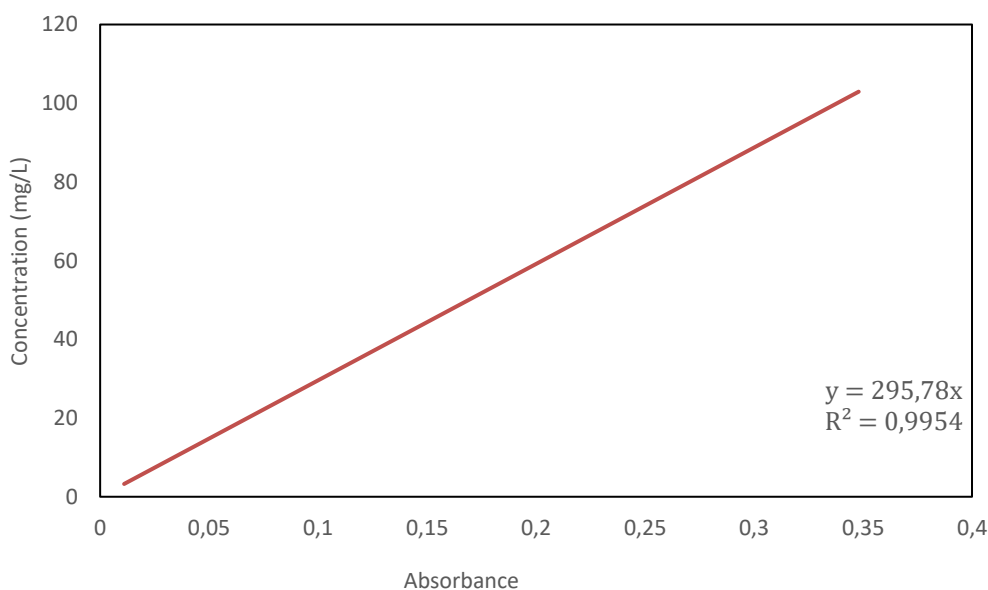


Figure 1: Calibration curve for VY4 dye at 419 nm.

3.2 Characterisation results of the adsorbent

The RSSC was found to have a high percentage fixed carbon of 82.54 %, surface area of 999 m²/g, iodine number of 878 mg/g, moisture content of 3.0 %, volatile matter content of 12.32 %, and bulk density of 0.55 g/cm². Larger surface area entails a greater adsorption capacity [46]. The RSSC sample was found to have a low ash content of 5.14 %. High ash content may interfere with the pore structure of the sorbent material and will result in low adsorption [47]. Bulk density is an important parameter of powdered solids. Bulk density specifies the fibre content of a material [48]. The American Water Work Association, AWWA has established a lower limit on bulk density at 0.55 gm/ml for activated carbon [47]. The bulk density value of 0.55 g/cm² implies that the RSSC can be a potential adsorbent. The pH of 6.8 obtained for RSSC is near neutral which will be useful for the management of wastewater and the purification of drinking water [48]. The XRF analysis of the RSSC indicates the existence of high percentage of minerals including potassium oxide (K₂O, 8.2 %), iron oxide (Fe₂O₃, 29.9 %), silicon oxide (SiO₂, 21%), and calcium oxide (CaO, 16.9 %). The presence of these minerals will favor the process of ion adsorption [49]. The SEM image of RSSC (4000x) is shown in Fig. 2. High porosity was observed on the RSSC (Fig. 2). The FTIR spectra on RSSC is shown in Fig. 3.

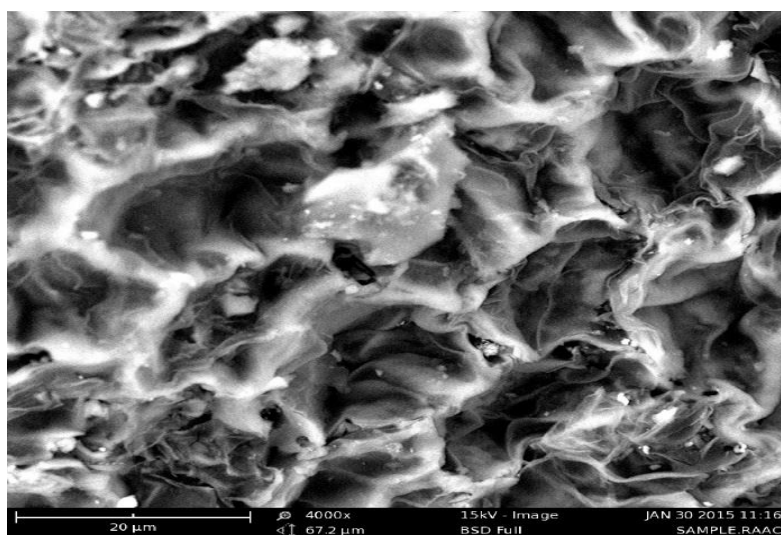


Figure 2: SEM image of RSSC.

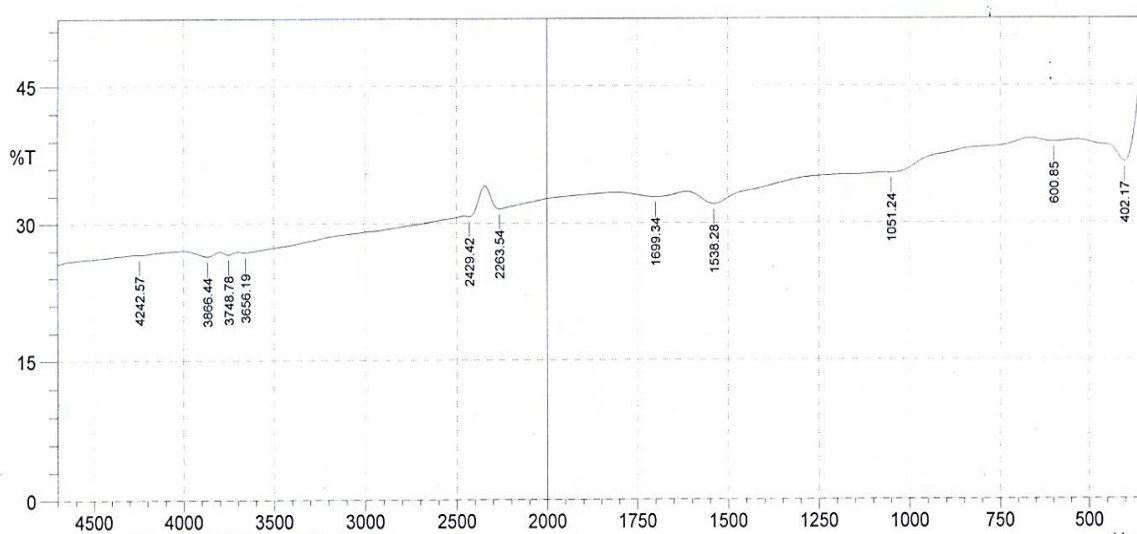


Figure 3: FTIR spectra of RSSC.

The presence of C – Cl stretching of alkyl halides (600.85 cm^{-1}), C – N stretching of aliphatic amines (1051.24 cm^{-1}), N – O asymmetric stretching of nitro compounds (1538.28 cm^{-1}), C=O stretching of amides, ketones, aldehydes, carboxylic acid, esters (1699.34 cm^{-1}), - C \equiv C – stretching of alkynes (2263.54 and 2429.42 cm^{-1}) and O – H stretching of alcohols and phenols (3656.19 , 3748.78 and 3866.44 cm^{-1}) were observed on the RSSC. This O–H bond participated actively in the adsorption of VY4 because of the existence of the hydrogen bonding [50, 51].

3.3 The influence of pH

All the samples were treated for an hour at pHs of 2, 4, 6, 8, and 10 at room temperature (303 K). The ionization degree of species is influenced by the pH, which in turn, affects the sorption process. The pH of the solution determines the sorbent's surface charge and the state of adsorbate in suspension [53]. The removal of the VY4 was highly dependent on pH (as seen in Fig. 4). The carbon will have a net positive charge at low values of pH. Higher uptakes achieved at lower pH may be owing to the electrostatic attractions among the functional/chemical groups (which is negatively charged) found on the reactive dye and the RSSC surface (which is positively charged). Hydrogen ion as well functions as a bridging ligand in between the dye molecule and the wall of the biosorbent [54].

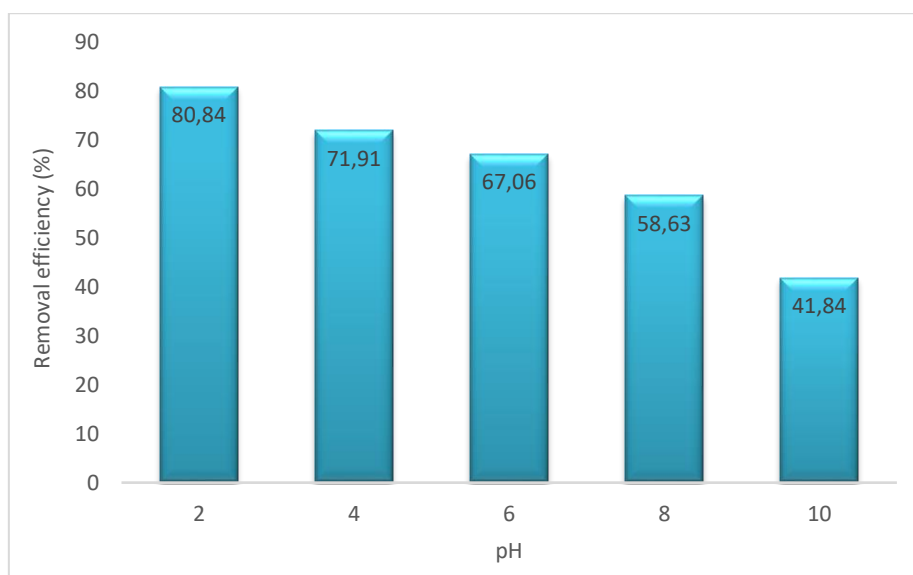


Figure 4: The influence of pH on the removal of VY4 using RSSC (conditions: dosage of RSSC = 1.0 g, concentration of VY4= 100 mg/L, interaction time = 60 min, temperature = 303 K).

3.4 The influence of RSSC dose

Figure 5 explains the influence of RSSC dosage on VY4 removal. The %removal improved as the RSSC dose was increased. The number of active adsorption sites available for VY4 elimination was improved with rising dosage [47, 55]. VY4 removal nearly became constant as RSSC dose was increased from 1.0 to 2.0 g; this may be due to overlapping of the RSSC particles and the RSSC sites remaining unsaturated throughout the VY4 removal process [56]. Mahmoud et al. [57] obtained a similar result.

3.5 The influence of temperature

Figure 6 shows that the %removal slightly improved with rising temperature (303 – 323 K), which gave optimum removal of 82.71 %. Therefore, higher temperatures facilitated the VY4 removal to an extent [20] and started declining (82.71 -78.31 %) as the temperature was raised further from the temperature of 323 to 343 K. This is because at very high temperature the biosorbent loses its property due to

denaturation [58]. But the temperature of 303 K (room temperature) was chosen as the optimum temperature instead of 323 K since the removal efficiency increased by approximately 2 %, so there's no need of wasting more energy for just improving the efficiency by 2 %.

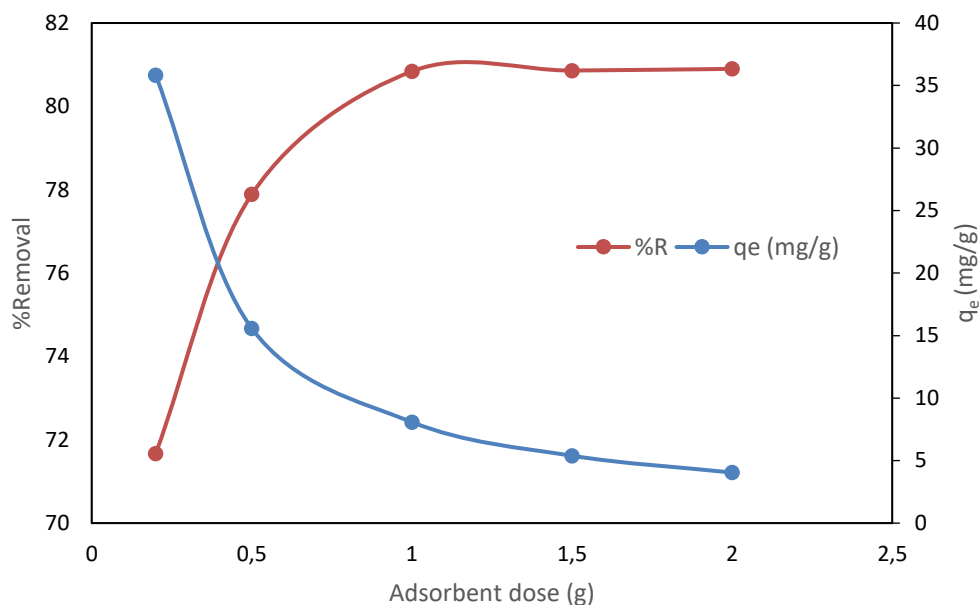


Figure 5: Influence of RSSC dosage on VY4 removal using RSSC (conditions: VY4 concentration = 100 mg/L, pH = 2, interaction time = 60 min, temperature = 303 K).

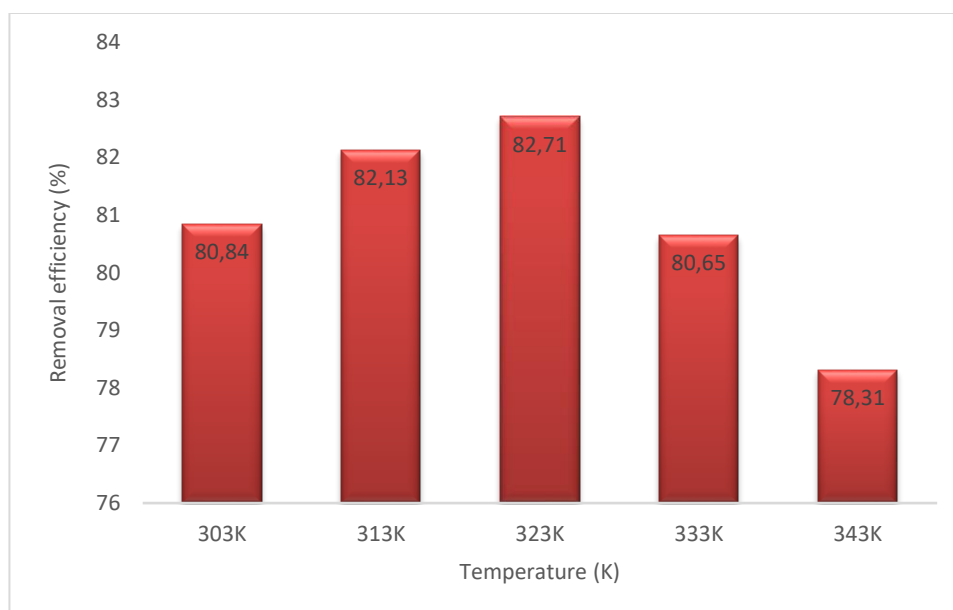


Figure 6: Influence of temperature on VY4 removal using RSSC (conditions: pH =2, dosage of RSSC = 1.0 g, concentration of VY4 = 100 mg/L, interaction time = 60 min).

3.6. The influence of VY4 concentration

The impact of VY4 concentration was examined in the range of 100–500 mg/L (Fig. 7). The %removal of the adsorbates declined as VY4 concentration increased during VY4 reduction via RSSC. VY4 elimination is highly reliant on VY4 concentration [59]. A similar observation was made by Alzaydien [60]. An increase in VY4 concentration caused RSSC to be highly saturated resulting in lower dye removal.

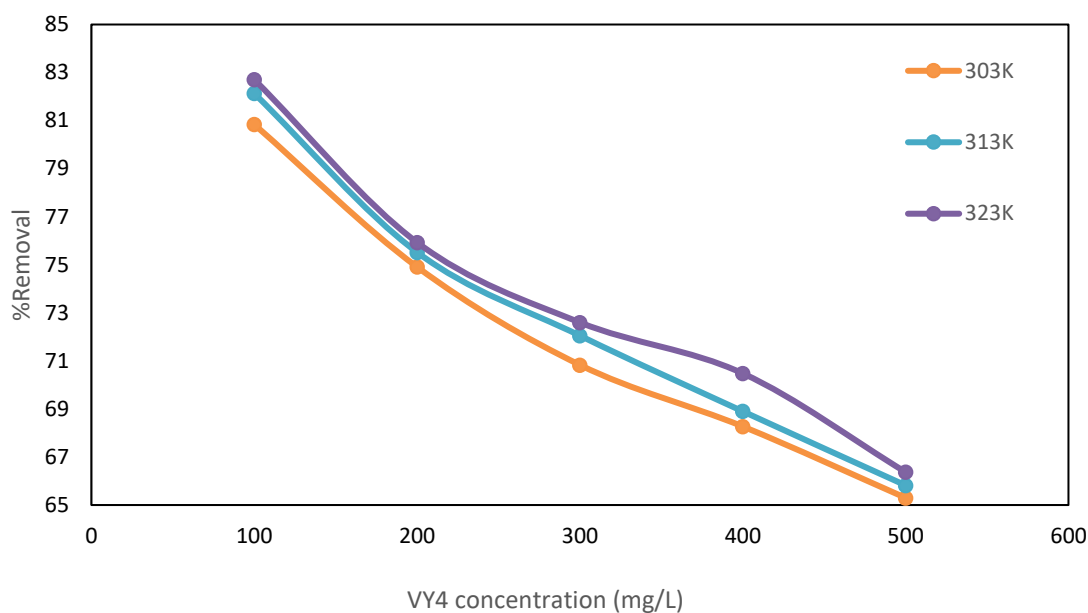


Figure 7: The influence of VY4 concentration on VY4 removal using RSSC (conditions: pH =2, RSSC dosage = 1.0 g, interaction time = 60 min).

3.7 The influence of interaction time

The impact of interaction time on VY4 removal onto RSSC was examined at 10, 20, 30, 45, 60, 90, 120, and 150 min. From Fig. 8, the %removal improved with rising interaction time. An increase in interaction time will increase dye mobility during the sorption process [2]. The rate of VY4 removal was higher initially owing to the large surface area of the RSSC available and after some time, little improvement in the dye uptake was observed since there are few active adsorption sites on the RSSC surface [61]. Equilibrium was achieved at 90 min. Similar observations were made by Meroufel et al. [62] and Idris et al. [40].

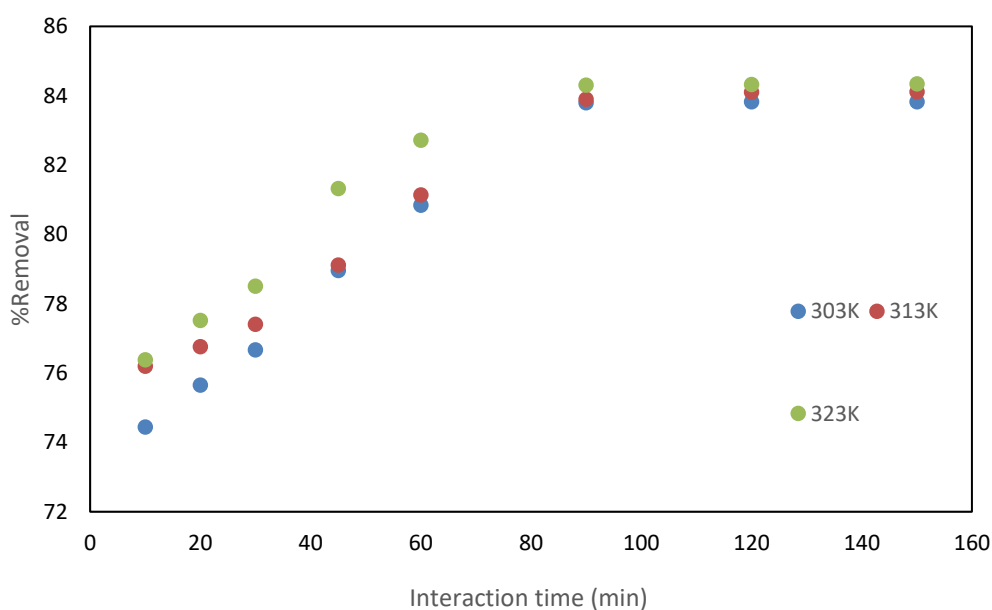


Figure 8: Effect of interaction time on the removal of VY4 using RSSC (conditions: pH =2, RSSC dosage = 1.0 g, concentration = 100 mg/L).

3.8. Adsorption isotherms

Generally, isotherms offer significant facts in optimizing the use of adsorbents [63]. The adsorption experiments were performed at 303 K at different VY4 concentrations of 100, 200, 300, 400, and 500 mg/L using 1.0 g of RSSC at a contact time of 90 min and stirring speed of 120 rpm. The Langmuir, Freundlich, and Temkin isotherm models were used to fit the isotherm data using the Microsoft Excel software. The Dubinin-Radushkevich (D-R) isotherm was also employed because it is more general than the above-mentioned isotherms; the apparent adsorption energy can be ascertained [64]. Based on this energy of sorption (E) one can predict whether an adsorption process is chemisorptions or physisorptions. The adsorption is physisorption or chemisorptions in nature if the energy of activation is < 8 kJ/mol or between 8 and 16 kJ/mol [52, 65, 66]. Also, the linear and nonlinear forms of isotherm models used to describe the isotherm data are presented in Table 2 [46, 53, 55, 62, 67-71]. The nonlinear plots of the isotherm models are shown in Fig. 9. The value of the correlation coefficient (R^2) was used to test the model that best describes the model. Also, in order to further validate the nonlinear isotherm models with the experimental results, the error functions: root mean squared error (RMSE) and Chi-square (χ^2) were used. The use of only the R^2 for the validation of nonlinear isotherm data analysis is not sufficient enough, because the experimental results may have high R^2 value.

Table 2: Isotherm models employed to fit VY4 adsorption by RSSC.

Isotherm model	Nonlinear equation	Linear equation	Description of parameters
Langmuir	$q_e = \frac{q_m K_L C_e}{1 + K_L C_e}$	$\frac{C_e}{q_e} = \frac{1}{q_m K_L} + \frac{C_e}{q_m}$	q_m = maximum monolayer adsorption capacity (mg/g), and K_L = Langmuir constant which is related to the heat of adsorption (L/mg).
Freundlich	$q_e = K_F C_e^{\frac{1}{n}}$	$\text{Log } q_e = \frac{1}{n} \text{Log } C_e + \text{Log } K_F$	K_F = Freundlich isotherm constant (L/g), n = the magnitude of favorability of adsorption, and q_e = amount of adsorbate adsorbed at equilibrium (mg/g).
Temkin	$q_e = \frac{RT}{B_T} \ln(A_T)(C_e)$	$q_e = B_T \ln A + B_T \ln C_e$	q_e = amount of adsorbate adsorbed on adsorbent at equilibrium (mg/g), A = Temkin constant and B_T = constant associated with the heat of adsorption which is defined as $B=RT/b$
Dubinin-Radushkevich (D-R)	$q_e = q_D \exp(-B\varepsilon^2)$ $\varepsilon = RT \ln(1+1/C_e)$ $E = 1/(2B)^{\frac{1}{2}}$	$\text{Ln } q_e = \text{Ln } q_D - B\varepsilon^2$	q_D = theoretical saturation capacity (mg/g), B = constant related to mean free energy of adsorption per mole of the adsorbate (mol^2/J^2), ε = Polanyi potential which is associated with equilibrium, R is the universal gas constant (8.314 J/mol/K), T = temperature in Kelvin and E = mean sorption energy (kJ/mol)

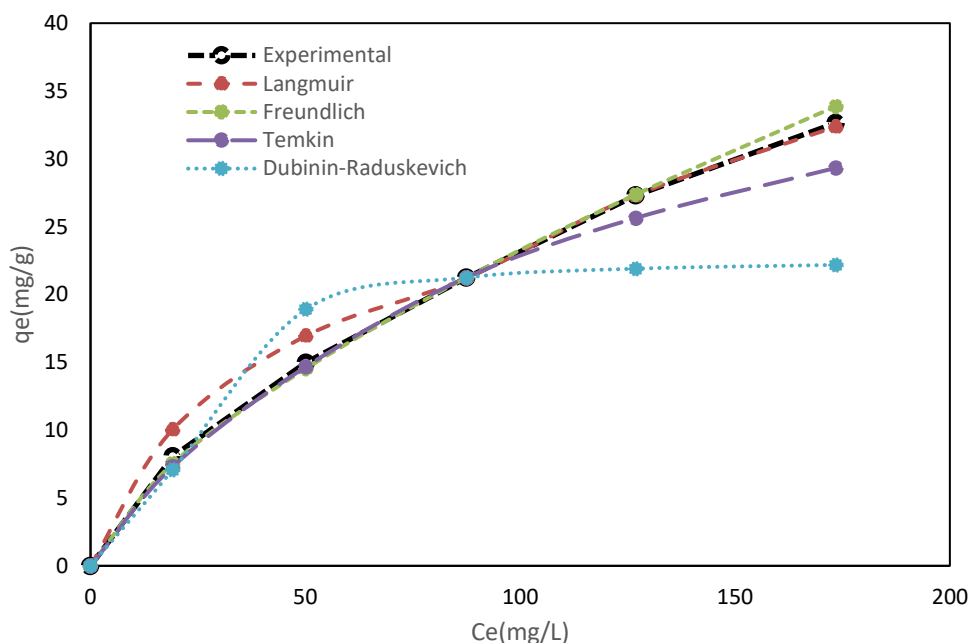


Figure 9: Nonlinear isotherm fits for VY4 adsorption onto RSSC at 303 K (conditions: pH = 2, RSSC dosage = 1.0 g, concentration = 100 mg/L, temperature = 303 K).

Therefore, it is necessary to diagnose the result of regression for residue analysis. A lower value of RMSE and χ^2 shows a better fit. The RMSE and χ^2 were evaluated using equations (3) and (4), respectively [64, 72]:

$$RMSE = \sqrt{\frac{1}{p-2} \sum_{i=1}^p (q_{e,exp} - q_{e,cal})^2} \quad (3)$$

$$\chi^2 = \sum_{i=1}^N \frac{(q_{e,exp} - q_{e,cal})^2}{q_{e,cal}} \quad (4)$$

Where $q_{e,cal}$ is the value that is computed from the model fit, $q_{e,exp}$ is calculated from test elements and p is the number of parameters in the model.

The dimensionless separation factor, R_L is given by Eq. (5) [45, 73]:

$$R_L = \frac{1}{1 + K_L C_0} \quad (5)$$

The R_L value indicates whether the isotherm is either favorable ($0 < R_L < 1$), unfavorable ($R_L > 1$), linear ($R_L = 1$) or irreversible ($R_L = 0$) [74].

The VY4 adsorption data conformed to more to the Freundlich model with regards to its correlation coefficient, R^2 (Table 3). Also, the low values of RMSE and χ^2 indicate that the Freundlich model gave a better fit to the isotherm results. The Freundlich model assumes a heterogeneous surface [75] and multilayer adsorption [76]. Also, its fit into the Freundlich model signifies a chemisorption process [76]. Monolayer sorption capacity, q_m of 27.546 mg/g was obtained from the nonlinear fit of the Langmuir model. R_L value of 0.011 was estimated for the VY4 removal onto RSSC, implying that the process is favorable for Langmuir prevailed process. The parameter, n provides the intensity of adsorption; if the n values are in the range of $0.1 < 1/n < 0.5$, it indicates that good adsorption is promising, $0.5 < 1/n < 1$ indicates moderate adsorption and $1/n > 1$ indicates weak adsorption [36]. The $1/n$ -value, 0.6813 (Table 3) indicates moderate adsorption [78]. Also, the mean energy of sorption, E value was estimated as 0.0844 kJ/mol through the D-R, suggesting that VY4 removal on RSSC is a chemisorption process since the value was found to be less than 8 kJ/mol [52].

Table 3: Nonlinear isotherm parameters for VY4 adsorption onto RSSC at 303 K (conditions: pH = 2, RSSC dosage = 1 g, concentration = 100 mg/L).

Langmuir	Freundlich	Temkin	Dubinin-Radushkevich
$q_m = 27.546 \text{ mg/g}$	$1/n = 0.6813$	$B_T = 2.1043 \text{ J/mg}$	$q_D = 22.50827112 \text{ mg/g}$
$K_L = 0.9112 \text{ L/mg}$	$K_F = 1.0144 \text{ L/g}$	$A = 0.0691$	$B = 7.02 \times 10^{-5} \text{ mol}^2/\text{kJ}^2$
$R^2 = 0.9718$	$R^2 = 0.9999$	$R^2 = 0.9855$	$R^2 = 0.8436$
$\text{RMSE} = 2.6385$	$\text{RMSE} = 0.033$	$\text{RMSE} = 0.8350$	$\text{RMSE} = 2.7055$
$= 0.4320\chi^2$	$= 0.0443\chi^2$	$= 0.3755\chi^2$	$= 4.9430\chi^2$

3.9 Kinetics of adsorption

These kinetic models are useful for the design and optimization of effluent management processes. The experiments were carried out by taking 100 mL samples of dyes (concentration: 100 mg/L) in separate flasks and treated with 1.0 g of adsorbent dose at different interaction times of 10, 20, 30, 45, 60, 90, 120 and 150 min at 120 rpm agitation speed. The sorption capacity at time t , q_t (mg/g) was obtained as Eq. (6):

$$q_t = \frac{(C_0 - C_t)V}{W} \quad (6)$$

Where C_0 and C_t (mg/L) were the liquid-phase concentrations of solute at $t = 0$ and at a given time t . V is the adsorbate solution volume and W is the mass of RSSC used (g).

The kinetic data obtained experimentally were fitted into the nonlinear Lagergren pseudo-first-order (PFO) and Ho/Mckay pseudo-second-order (PSO) models presented in Table 4 [6, 50, 55, 76, 79]. The R^2 was used as the basis to determine which model best described the kinetic data. The applicability of the kinetic model to describe the adsorption process, apart from the regression coefficient (R^2) was further validated using the error functions, Marquardt's percent standard deviation (MPSD), hybrid error function (HYBRID), sum of the errors squared (ERRSQ), average relative error (ARE), and normalized standard deviation ($\Delta q(\%)$) stated below as equations [64, 76]:

$$\text{MPSD} = 100 \sqrt{\frac{1}{n-p} \sum_{i=1}^n \left(\frac{q_{e,exp} - q_{e,calc}}{q_{e,exp}} \right)_i^2} \quad (7)$$

$$\text{HYBRID} = \frac{100}{n-p} \sum_{i=1}^n \left[\frac{(q_{e,exp} - q_{e,calc})^2}{q_{e,exp}} \right]_i \quad (8)$$

$$\text{ERRSQ} = \sum_{i=1}^p (q_{e,exp} - q_{e,calc})^2 \quad (9)$$

$$\text{ARE} = \frac{100}{n} \sum_{i=1}^N \left| \frac{q_{e,exp} - q_{e,calc}}{q_{e,exp}} \right|_i \quad (10)$$

$$\Delta q(\%) = 100 \sqrt{\frac{\sum (q_{e,exp} - q_{e,calc})^2 / q_{e,exp}^2}{n-1}} \quad (11)$$

Where $q_{e,exp}$ and $q_{e,calc}$ (mg/g) are the experimental and calculated amounts of colour adsorbed, respectively; n is the number of measurements made and p is the number of the test elements.

The smaller MPSD, HYBRID, ARE, ERRSQ, and $\Delta q(\%)$ values indicate a more accurate estimation of q_e value. HYBRID and MPSD error functions were used in addition to R^2 because the number of parameters in the regression model (that is, p parameter) is effective in them [76].

The nonlinear PFO and PSO kinetic plots are in Fig. 10. The calculated PFO and PSO parameters are shown in Table 5. The adsorption phenomenon was best described by the PFO than the PSO model at all temperatures considering the values of R^2 and the error functions (Table 5).

Table 4: Kinetic models employed to fit VY4 adsorption by RSSC.

Kinetic model	Nonlinear equation	Linear equation	Description of parameters
Pseudo-first-order	$q_t = q_e[1 - \exp(-K_1 t)]$	$\text{Log}(q_e - q_t) = \text{Log } q_e - \frac{K_1}{2.303} t$	K_1 = pseudo- first-order rate constant (min^{-1}); q_e = amount of adsorbate adsorbed at equilibrium (mg/g); q_t = amount of adsorbate adsorbed at time t (mg/g)
Pseudo-second-order	$q_t = \frac{K_2 q_e^2 t}{1 + q_e k_{2p} t}$	$\frac{t}{q_t} = \frac{1}{K_2} + \frac{1}{q_e} t$	K_2 = pseudo-second order rate constant (g/mg min); q_e = amount of adsorbate adsorbed at equilibrium (mg/g); q_t = amount of adsorbate adsorbed at time t (mg/g)

Table 5. Kinetic parameters obtained for the adsorption of VY4 on RSSC (conditions: pH = 2, RSSC dosage = 1.0 g, concentration = 100 mg/L).

Kinetic Model	Temperature (K)		
	303	313	323
Pseudo-first-order			
k_1 (min^{-1})	0.1069	0.1069	0.1072
q_e (mg/g)	7.9951	7.9987	7.9993
R^2	0.9990	0.9989	0.9998
ERRSQ	0.0009	0.0256	0.0829
HYBRID	0.0003	0.0047	0.5623
MPSD	1.5097	1.5197	14.434
ARE	0.1453	0.1463	1.3889
Δq (%)	1.1206	2.8242	8.7039
Pseudo-second-order			
k_2 (g/mg/min)	0.9974	0.9974	0.9971
q_e (mg/g)	7.9222	7.9322	7.9522
R^2	0.9956	0.9994	0.9905
ERRSQ	0.0304	0.0378	0.1119
HYBRID	0.6559	0.6552	0.7089
MPSD	0.9617	0.3242	1.4068
ARE	0.0925	0.0312	0.1354
Δq (%)	0.4224	1.3045	2.7173

Fitting of an intra-particle diffusion plot is the most common method used for the identification of the mechanism involved in an adsorption process. Weber and Morris proposed that intra-particle diffusion is expressed as [45, 67]:

$$q_t = k_{pi} t^{0.5} + c \quad (12)$$

where c is a constant that provides an idea about the thickness of the boundary layer, k_{pi} is the intraparticle diffusion rate constant ($\text{mg/g min}^{0.5}$) and q_t is the amount adsorbed (mg/g) at time t (min). k_{pi} and c were obtained from the slope and intercept of the straight-line plot of q_t versus $t^{0.5}$ (Fig. 11), respectively.

The intraparticle diffusion parameters and the R^2 values obtained for the VY4 adsorption onto RSSC at different temperatures are presented in Table 6. The R^2 values indicate that the intraparticle diffusion model was able to explain the data indicating that the process was been controlled by intraparticle diffusion. The k_{pi} and c values were improved with rising solution temperature. Also, the plot of q_t versus $t^{0.5}$ did not surpass the origin inferring that the intraparticle diffusion is not solely the rate-limiting step [81]. This deviance from the origin is owing to the change in the rate of mass transfer in the initial and final sorption stages [39].

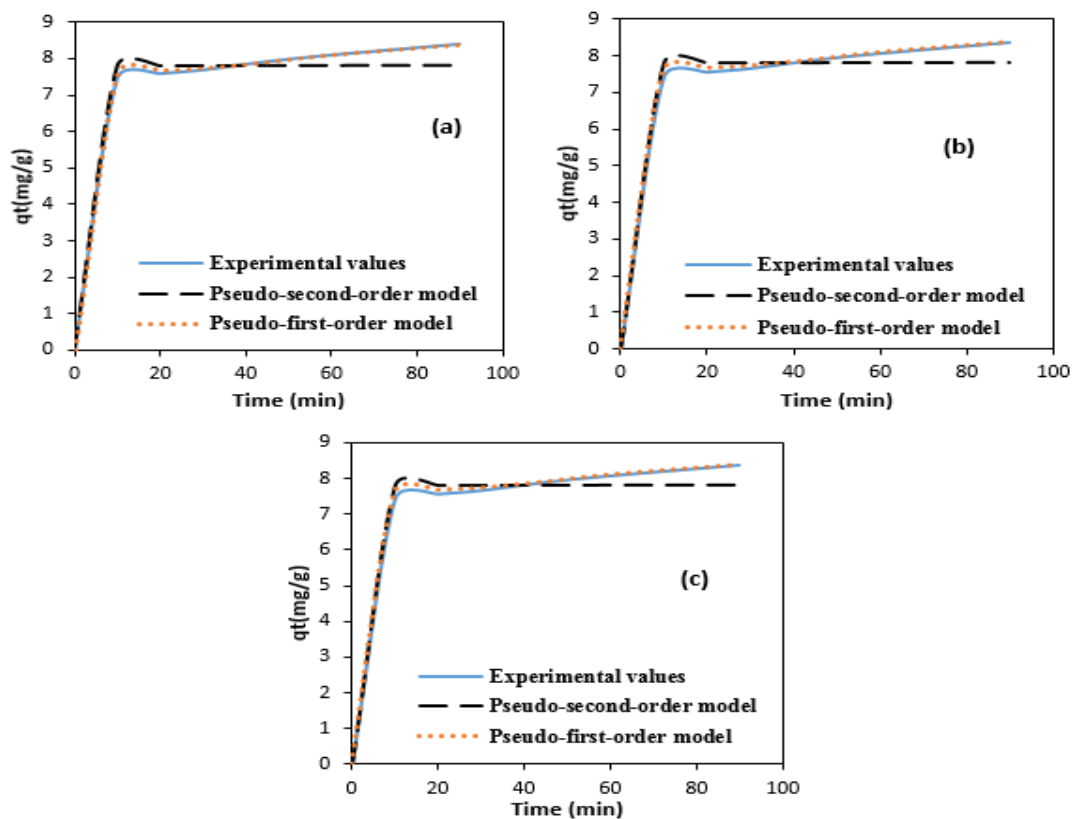


Figure 10. Nonlinear fits at (c) 303, (d) 313, and (e) 323 K for VY4 adsorption onto RSSC.

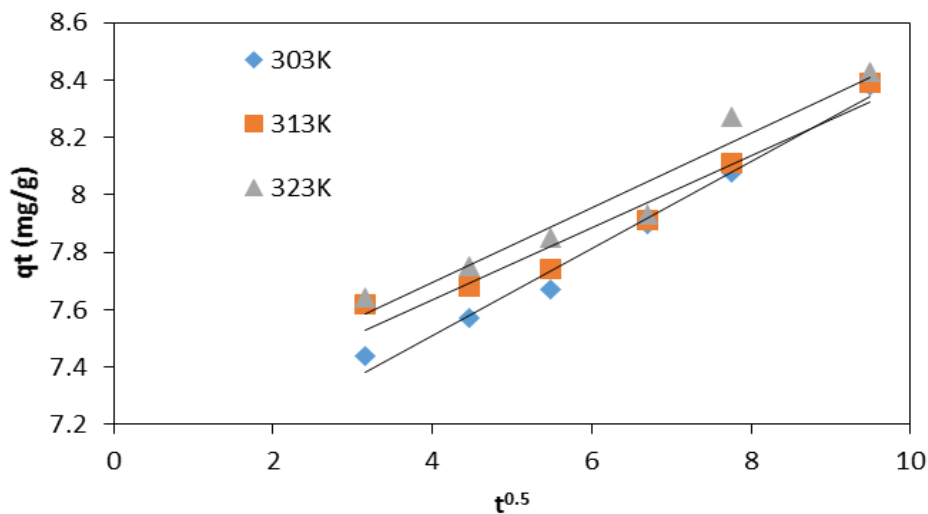


Figure 11: Intraparticle diffusion plots of VY4 adsorption onto RSSC.

Table 6: Intraparticle diffusion parameters obtained for the adsorption of VY4 on RSSC (conditions: pH = 2, RSSC dosage = 1.0 g, concentration = 100 mg/L).

Intra particle and film diffusion parameters	Temperature (K)		
	303	313	323
k_{pi} (mg g ⁻¹ min ^{-0.5})	0.151	0.125	0.130
c	6.901	7.133	7.171
R^2	0.984	0.946	0.944

3.10 Activation energy and Thermodynamic studies

The energy of activation of the VY4 removal onto RSSC can be estimated using the Arrhenius equation [82, 83]:

$$\ln k_2 = \ln A - \frac{E_a}{RT} \quad (13)$$

Where k_2 is the pseudo-second-order kinetic constant (g/mg h), E_a is the activation energy of adsorption (kJ/mol), R is 8.314 J/mol K and A is the Arrhenius factor. E_a can be calculated from the linear plot of $\ln k_2$ versus $1/T$ (not shown).

The magnitude of the energy of activation can be applied as a basis to differentiate between chemical and physical adsorption processes. For physical adsorption reactions, the energy of activation required is ranging from 5-40 kJ/mol while chemical adsorption requires larger activation energies (40–800 kJ/mol) [50]. The value of activation energy, E_a calculated for VY4 adsorption on RSSC for VY4 is 94.7197 kJ/mol. The activation energy of adsorption of VY4 on RSSC is greater than 40 kJ/mol which implies that the rate-limiting step might be a chemically controlled process.

The thermodynamic free energy change parameter, ΔG^0 (standard), ΔH^0 (standard enthalpy), and ΔS^0 (standard entropy) were determined at temperatures of 303, 313, and 323 K. The values of ΔH^0 and ΔS^0 can be obtained from Eq. (14) [19, 84]:

$$\ln K_L = \frac{\Delta S^0}{R} - \frac{\Delta H^0}{RT} \quad (14)$$

where R (8.314 J/mol K) is the universal gas constant, T (K) is the solution temperature and K_L (L/mg) is the Langmuir isotherm constant.

The Gibbs free energy change, ΔG^0 can be calculated using Eq. (15) [22, 76]:

$$\Delta G^0 = \Delta H^0 - T\Delta S^0 \quad (15)$$

The values of ΔG^0 calculated were found to be negative for the adsorption of VY4 dye on RSSC at all studied temperatures (Table 7). ΔG^0 is used to measure the spontaneity of an adsorption process [85]. The values of ΔG^0 were found to decline with increasing temperature (Table 7) which means that the adsorption of VY4 on RSSC is favourable and spontaneous [86]. The values of ΔH^0 and ΔS^0 (Table 7) were calculated from the Vant Hoff plots (Fig. 12) plots of $\ln K_L$ versus $1/T$. The positive value of ΔH^0 suggests that the process is endothermic in nature [87]. The negative value of ΔG^0 indicates that the adsorption process is spontaneous and favourable. The negative value of ΔS^0 indicates that the measure of freedom at the solid-solution level drops during the adsorption process [88].

Table 7: Thermodynamic parameters obtained for VY4 adsorption on RSSC.

T (K)	$1/T$ (K ⁻¹)	k_L (g/mg min)	$\ln k_L$	ΔG^0 (kJ/mol)	ΔH^0 (kJ/mol)	ΔS^0 (J/K/mol)
303	3.30 x 10 ⁻³	0.0079	-4.8409	-7.665		
313	3.19 x 10 ⁻³	0.0085	-4.7677	-7.918	4.524	-25.283
323	3.10 x 10 ⁻³	0.0088	-4.7330	-8.171		

3.11 Comparison of VY4 dye removal with other pollutants using rubber seed shells

Table 8 shows the comparison of VY4 removal with other dyes using rubber seed shells (RSS). The monolayer adsorption capacity (q_m), maximum removal efficiency, and optimum pH obtained using RSS on different pollutants are presented in Table 8. It can be confirmed that the RSS can be utilized as a viable adsorbent for the removal of different types of pollutants. The biosorbent was also found to be good for VY4 dye specifically when compared with other adsorbents in terms of its maximum removal efficiency and monolayer adsorption capacity.

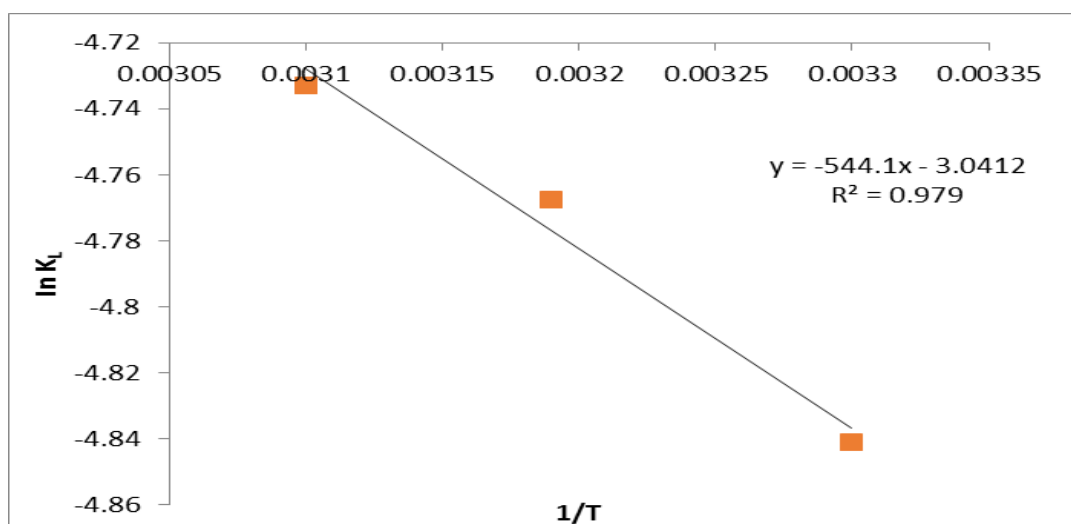


Figure 12: Van't Hoff plot of VY4 adsorption on RSSC.

Table 8: Comparison of VY4 removal with other pollutants using rubber seed shells

Dye	Adsorbent	pH	q_m (mg/g)	Maximum (%) removal	Reference
Methylene blue	Rubber seed shells	-	82.64	-	[37]
Malachite green	Rubber seed coat	6	72.73	-	[40]
Congo red	Rubber seed shells	Between 5 and 6	9.82	90	[41]
Rhodamine B	Rubber seed shells	3	3.185	99.52	[42]
Crystal violet	Rubber seed shells	Not adjusted	23.81	-	[89]
Vat yellow 4	Rubber seed shells	2	27.55	84.34	Present study
Vat yellow 4	H ₃ PO ₄ treated velvet beans	2	34.48	98.71	[6]
Vat yellow 4	NaCl-treated velvet beans	2	52.63	96.63	[6]
Vat yellow 4	Terminalia superba sawdust	Not adjusted	12.658	68	[10]

Conclusion

The adsorptive removal of VY4 on activated Rubber seed shells carbon (RSSC) has been studied. The optimal conditions of the adsorption process were investigated. Also, the kinetics, isotherm, and thermodynamics of the adsorption process were studied. High percentage fixed carbon percentage of 82.54% and surface area of 999 m²/g were observed on the RSSC. The SEM analysis revealed the high porosity of the RSSC. The XRF analysis indicated the presence of minerals (K₂O = 8.2 %, Fe₂O₃ = 29.9 %, SiO₂ = 21 %, and CaO = 16.9 %) which will favour the process of ion adsorption. The process was improved with increasing RSSC dosage, interaction time, and temperature. Higher removal was obtained at the lowest pH studied. Optimal conditions of interaction time: 90 min, temperature: 303 K, initial pH: 2, and RSSC dose: 1.0 g led to 84.34% elimination with maximum adsorption capacity (q_m) of 27.55 mg/g. The dimensionless separation factor ($R_L = 0.011$) has shown that the RSSC can be used for the

removal of VY4 from its aqueous solution. The values of the coefficient of determination (R^2) and error functions indicate that the process was best described by the pseudo-first-order kinetic and Freundlich isotherm models than the other models. Also, the process was found to be favourable, spontaneous, and endothermic in nature. The prepared Rubber seed shell carbon can be utilized for the removal of VY4 from aqueous environments.

References

1. T. Santhi, S. Manonmani, T. Smitha, Kinetics and isotherm studies on cationic dyes adsorption onto *Annona squamosa* seed activated carbon, *International Journal of Engineering Science and Technology* 2(3) (2010) 287-295.
2. A. Abbas, S. Murtaza, K. Shahid, M. Munir, R. Ayub, S. Akber, Comparative study of adsorptive removal of congo red and brilliant green dyes from water using peanut shell, *Middle-East J. Sci. Res.* 11 (2012) 828-832.
3. Y. S. Al-Degs, M. I. El-Barghouthi, A. H. El-Sheikh, G. M. Walker, Effect of solution pH, ionic strength, and temperature on adsorption behavior of reactive dyes on activated carbon, *Dyes and Pigments* 2(3) (2007) 1997-2004. <https://doi.org/10.1016/j.dyepig.2007.03.001>
4. L.S. Tan, K. Jain, C.A. Rozaini, Adsorption of textile dye from aqueous solution on pretreated mangrove bark, an agricultural waste: equilibrium and kinetic studies, *Journal of Applied Sciences in Environmental Sanitation*, 5 (3) (2010) 283-294.
5. D.K. Mahmoud, M.A.M. Salleh, W.A.W.A. Karim, A. Idris, Z.Z. Abidin, Batch adsorption of basic dye using acid treated kenaf fibre char: equilibrium, kinetic and thermodynamic studies, *Chem. Eng. J.* 181–182 (2012) 449–457. <https://doi.org/10.1016/j.cej.2011.11.116>
6. C.A. Igwegbe, O.D. Onukwuli, J.T. Nwabanne, Adsorptive removal of vat yellow 4 on activated *Mucuna pruriens* (velvet bean) seed shells carbon, *Asian J. Chem. Sci.* 1 (2016) 1–16. <https://doi.org/10.9734/AJOCS/2016/30210>
7. M. Kaykhahi, M. Sasani, S. Marghzari, Removal of dyes from the environment by adsorption, *Proc. Chem. Mater. Eng.* 6 (2018) 31-35. DOI: [10.13189/cme.2018.060201](https://doi.org/10.13189/cme.2018.060201)
8. V.K. Gupta, Suhas, Application of low-cost adsorbents for dye removal – A review, *J. Environ. Manage.* (2009) 2313-2342. <https://doi.org/10.1016/j.jenvman.2008.11.017>
9. I. Chaari, F. Jamoussi Application of activated carbon for vat dye removal from aqueous solution, *J. App. Sci. Environ. Sanit.* 6 (2011) 247-256.
10. M. Badu, I.W. Boateng, N.O. Boadi, Evaluation of adsorption of textile dyes by wood sawdust, *Res. J. Phys. Appl. Sci.* 3 (2014) 006–014. <http://hdl.handle.net/123456789/11206>
11. T.A. Khan, S. Sharma, I. Ali, Adsorption of Rhodamine B dye from aqueous solution onto acid activated mango (*Magnifera indica*) leaf powder: Equilibrium, kinetic and thermodynamic studies, *Journal of Toxicology and Environmental Health Sciences* 3(10) (2011) 286–297.
12. N.S. Maurya, A. K. Mittal, P. Cornel, Evaluation of adsorption potential of adsorbents: a case of uptake of cationic dyes, *Journal of Environmental Biology* 29(1) (2008) 31-36.
13. I.A. Obiora-Okafo, O.D. Onukwuli, Optimization of coagulation-flocculation process for colour removal from azo dye using natural polymers: response surface methodological approach, *Nigerian J. Technol.* 36 (2017) 482–495.
14. M.R. Gadekar, M.M. Ahammed, Coagulation/flocculation process for dye removal using water treatment residuals: modelling through artificial neural networks, *Desal. Water Treat.* 57(55) (2016) 26392–26400. [doi:10.1080/19443994.2016.1165150](https://doi.org/10.1080/19443994.2016.1165150)

15. F.I. El-Hosiny, M.A. Abdel-Khalek, K.A. Selim, I. Osama, Physicochemical study of dye removal using electro-coagulation-flotation process, *Physicochem. Probl. Miner. Process.* 54 (2018) 321-333. DOI: <https://doi.org/10.5277/ppmp1825>
16. C.F. Uzor, J.T. Nwabanne, Removal of Orange-G, Vat Yellow, Erythrosine dyes from synthetic wastewater by electrocoagulation and nanofiltration, *J. Adv. Chem. Eng.* 4 (2014) 3. DOI: [10.4172/2090-4568.1000112](https://doi.org/10.4172/2090-4568.1000112)
17. E. Pajootan, M. Arami, N.M. Mahmoodi, Binary system dye removal by electrocoagulation from synthetic and real colored wastewaters. *J. Taiwan Instit. Chem. Eng.* 43 (2012) 282-290. <https://doi.org/10.1016/j.jtice.2011.10.014>
18. A. Boukhemkhem, K. Rida, Improvement adsorption capacity of methylene blue onto modified Tamazert kaolin, *Adsorp. Sci. Technol.* 35 (2017) 9-10. doi.org/10.1177/0263617416684835
19. M. Rafiee, M. Jahangiri-rad, Adsorption of reactive blue 19 from aqueous solution by carbon nano tubes: equilibrium, thermodynamics and kinetic studies, *Res. J. Environ. Sci.* 8 (2014) 205-214. DOI: [10.3923/rjes.2014.205.214](https://doi.org/10.3923/rjes.2014.205.214)
20. G. Vijayakumar, R. Tamilarasan, M. Dharmendirakumar, Adsorption, kinetic, equilibrium and thermodynamic studies on the removal of basic dye Rhodamine-B from aqueous solution by the use of natural adsorbent perlite, *J. Mater. Environ. Sci.* 3 (1) (2012) 157-170.
21. C.A. Igwegbe, L. Mohammadi, S. Ahmadi, A. Rahdar, D. Khadkhodaiy, Dehghani R., Rahdar S., Modeling of adsorption of Methylene blue dye on Ho-CaWO₄ nanoparticles using Response surface methodology (RSM) and Artificial neural network (ANN) techniques, *MethodsX* 6 (2019) 1779-1797. <http://dx.doi.org/10.1016/j.mex.2019.07.016>
22. S. Ahmadi, A. Rahdar, S. Rahdar, C.A. Igwegbe, Removal of Remazol Black B from aqueous solution using P-γ-Fe₂O₃ nanoparticles: synthesis, physical characterization, isotherm, kinetic and thermodynamic studies, *Desal. Water Treat.* 152 (2019) 401-410. DOI: [10.5004/dwt.2019.23978](https://doi.org/10.5004/dwt.2019.23978)
23. S. Ahmadi, L. Mohammadi, C.A. Igwegbe, S. Rahdar, A.M. Banach, Application of response surface methodology in the degradation of Reactive Blue 19 using H₂O₂/MgO nanoparticles advanced oxidation process. *Inter. J. Ind. Chem.* 9 (2018) 241-253 <https://doi.org/10.1007/s40090-018-0153-4>
24. S. Ahmadi, C.A. Igwegbe, S. Rahdar, The application of thermally activated persulfate for degradation of Acid Blue 92 in aqueous solution. *Int. J. Ind. Chem.* 10 (2019) 249-260
25. S.K. Kavitha, P.N. Palanisamy, Photocatalytic degradation of Vat Yellow 4 using UV/TiO₂, *Modern Applied Science* 4(5) (2010) 130-142. DOI: [10.5539/mas.v4n5p130](https://doi.org/10.5539/mas.v4n5p130)
26. J.O. Ighalo, O.J. Ajala, G. Umenweke, S. Ogunniyi, C.A. Adeyanju, C.A. Igwegbe, A.G. Adeniyi, Mitigation of clofibric acid pollution by adsorption: A review of recent developments, *J. Environ. Chem. Eng.* 8(5) (2020) 104264. <https://doi.org/10.1016/j.jece.2020.104264>
27. C.A. Igwegbe, A.M. Banach, S. Ahmadi, Adsorption of Reactive Blue 19 from aqueous environment on magnesium oxide nanoparticles: kinetic, isotherm and thermodynamic studies, *The Pharmaceutical and Chemical Journal* 5 (2018) 111-121.
28. T. J. M. Fraga, M. N. Carvalho, M. G. Ghislandi, M. A. da Motta Sobrinho, Functionalized graphene-based materials as innovative adsorbents of organic pollutants: a concise overview, *Brazilian Journal of Chemical Engineering*, 36 (2019) 1-31
29. C.A. Onyechi, Textile wastewater treatment using activated carbon from agro wastes. M. Eng. Thesis. Department of Chemical Engineering, Nnamdi Azikiwe University, Awka, Nigeria (2014).

30. T.G. Venkatesha, R. Viswanatha, Y. Arthoba Nayaka, B.K. Chethana, Kinetics and thermodynamics of reactive and vat dyes adsorption on MgO nanoparticles, *Chem. Eng. J.* (2012) 198–199. <https://doi.org/10.1016/j.cej.2012.05.071>
31. M. Šmelcerović, D. Đorđević, M. Novaković, M. Mizdraković, Decolorization of a textile vat dye by adsorption on waste ash, *J. Serbian Chem. Soc.* 75(6) (2010) 855–872.
32. F. Amaringo, A. Hormaza, Optimization and evaluation of the indigo blue vat dye removal process on rice husk through statistical design, *Desal. Water Treat.* (2018) 253–260. DOI:10.5004/dwt.2018.22074
33. N. Tancredi, N. Medero, F. Möller, J. Píriz, C. Plada, T. Cordero, Phenol adsorption onto powdered and granular activated carbon, prepared from *Eucalyptus* wood, *J. Colloid Interface Sci.*, 279 (2004) 357–363. <https://doi.org/10.1016/j.jcis.2004.06.067>
34. S. Dinesh, Development and characterization of pellet activated carbon from new precursor. B. Tech. thesis, Department of Chemical Engineering, National Institute of Technology, Rourkela (2011).
35. U.A. Isah, A.I. Gatawa, A kinetic study of the adsorption of reactive yellow 21 dye on flamboyant shells activated carbon, *Advances in Applied Science Research* 3(6) (2012) 4036–4040.
36. M.A.M. Salleh, D.K. Mahmoud, W.A.W.A. Karim, A. Idris, Cationic and anionic dye adsorption by agricultural solid wastes: A comprehensive review, *Desalination* 280 (2011) 1–13. <https://doi.org/10.1016/j.desal.2011.07.019>
37. N.A. Oladoja, I.O. Asia, C.O. Aboluwoye, Y.B. Oladimeji, A.O. Ashogbon, Studies on sorption of basic dye by rubber (*Hevea brasiliensis*) seed shell, *Turkish Journal of Engineering and Environmental Science* 32 (2008) 143–152.
38. S. Rengaraj, S. Moon, R. Sivabalan, B. Arabindoo, V. Murugesan, Removal of phenol from aqueous solution and resin manufacturing industry wastewater using an agricultural waste: rubber seed coat, *J. Hazard. Mater.* 89(2-3) (2002) 185–96. [https://doi.org/10.1016/S0304-3894\(01\)00308-9](https://doi.org/10.1016/S0304-3894(01)00308-9)
39. S.E. Agarry, C.N. Owabor, Evaluation of the adsorption potential of rubber (*Hevea brasiliensis*) seed pericarp – activated carbon in abattoir wastewater treatment and in the removal of iron (II) ions from aqueous solution, *Nigerian Journal of Technology* 31 (2012) 346–358.
40. M.N. Idris, Z.A. Ahmad, M.A. Ahmad, Adsorption equilibrium of malachite green dye onto rubber seed coat based activated carbon, *International Journal of Basic & Applied Sciences* 11(3) (2011) 38–43.
41. M.A. Zulfikar, H. Setiyanto, Rusnadi, L. Solakhudin, Rubber seeds (*Hevea brasiliensis*): an adsorbent for adsorption of Congo red from aqueous solution, *Desal. Water Treat.* 56 (2015) 2976–2987. <https://doi.org/10.1080/19443994.2014.966276>
42. R.Y. Nadarajah, R. Mohammad, M. Mohamad, Rubber seed shells (*Hevea brasiliensis*): an adsorbent used for the removal of Rhodamine b dye, *ARPJ Journal of Engineering and Applied Sciences* 13(24) (2018) 9311–9317.
43. J.T. Nwabanne, P.K. Igbokwe, Thermodynamic and kinetic behaviours of lead (II) adsorption on activated carbon derived from palmyra palm nut, *J. Appl. Sci. Technol.* 2 (2012) 245–254.
44. C.A. Igwegbe, A.E. Al-Rawajfeh, H.I. Al-Itawi, S. Al-Qazaqi, E.A. Hashish, M. Al-Qatatsheh, S. Sharadqah, M. Sillanpaa, Utilization of calcined gypsum in water and wastewater treatment: removal of phenol, *Journal of Ecological Engineering* 20(7) (2019) 1–10. DOI: <https://doi.org/10.12911/22998993/108694>

45. S. Ahmadi, C.A. Igwegbe, Adsorptive removal of phenol and aniline by modified bentonite: adsorption isotherm and kinetics study, *Appl. Water Sci.* 8 (2018) 170. <https://doi.org/10.1007/s13201-018-0826-3>
46. N. Ayawei, A.N. Ebelegi, D. Wankasi, Modelling and interpretation of adsorption isotherms, *Journal of Chemistry* 3039817 (2017) 11 pages. <https://doi.org/10.1155/2017/3039817>
47. B.V. Devi, A.A. Jahagirdar, M.N.Z. Ahmed, Adsorption of chromium on activated carbon prepared from coconut shell, *Int. J. Eng. Res. App.* 2 (2012) 364-370.
48. J.R. Baseri, P.N. Palanisamy, P. Sivakumar, Preparation and characterization of activated carbon from *Thevetia peruviana* for the removal of dyes from textile waste water, *Adv. Appl. Sci. Res.* 3 (2012) 377-383.
49. F. Granados-Correa, J. Vilchis-Granados, M. Jiménez-Reyes, L.A. Quiroz-Granados, Adsorption behaviour of La(III) and Eu(III) Ions from aqueous solutions by hydroxyapatite: Kinetic, isotherm, and thermodynamic studies, *Journal of Chemistry* 2013, Article ID 751696 (2013) 9 pages. <https://doi.org/10.1155/2013/751696>
50. X. Zhang, X. Wang, Z. Chen, A novel nanocomposite as an efficient adsorbent for the rapid adsorption of Ni (II) from aqueous solution, *Materials* 10 (2017) 1124. doi: [10.3390/ma10101124](https://doi.org/10.3390/ma10101124)
51. F. Batool, J. Akbar, S. Iqbal, S. Noreen, S.N.A. Bukhari, Study of isothermal, kinetic, and thermodynamic parameters for adsorption of cadmium: an overview of linear and nonlinear approach and error analysis, *Bioinorganic Chemistry and Applications* 3463724 (2018) 11 pages. <https://doi.org/10.1155/2018/3463724>
52. A.A. Inyinbor, F.A. Adekola, G.A. Olatunji, Kinetics, isotherms and thermodynamic modeling of liquid phase adsorption of Rhodamine B dye onto *Raphia hookerie* fruit epicarp, *Water Resources and Industry* 15 (2016) 14–27. <https://doi.org/10.1016/j.wri.2016.06.001>
53. Z. Aksu, S. Tezer, Biosorption of reactive dyes on the green alga *Chlorella vulgaris*, *J. Process Biochem.* 40 (2005) 1347–1361
54. D. Pathania, S. Sharma, P. Singh, Removal of methylene blue by adsorption onto activated carbon developed from *Ficus carica* bast, *Arabian J. Chem.* 10 (2017) S1445-S1451. <https://doi.org/10.1016/j.arabjc.2013.04.021>
55. D. N. Taha, I. S. Samaka, L. A. Mohammed, Adsorptive removal of dye from industrial effluents using natural Iraqi palygorskite clay as low-cost adsorbent, *Journal of Asian Scientific Research* 3(9) (2013) 945-955.
56. D.K. Mahmoud, M.A.M. Salleh, W.A.W.A. Karim, A. Idris, Z.Z. Abidin, Batch adsorption of basic dye using acid treated kenaf fibre char: equilibrium, kinetic and thermodynamic studies, *Chem. Eng. J.* 181–182 (2012) 449–457. <https://doi.org/10.1016/j.cej.2011.11.116>
57. K.R. Rajesh, M. Rajasimman, N. Rajamohan, B. Sivaprakash, Equilibrium and kinetic studies on sorption of malachite green using *hydrilla verticillata* biomass, *Int. J. Environ. Res.* 4(4) (2010) 817-824.
58. P. Parimaladevi, V. Venkateswaran, Adsorption of cationic dyes (rhodamine B and methylene blue) from aqueous solution using treated fruit waste, *Journal of Applied Technology in Environmental Sanitation* 1 (3) (2011) 285-293.
59. A.S. Alzaydien, Adsorption of methylene blue from aqueous solution onto a low – cost natural Jordanian Tripoli, *American Journal of Applied Sciences*, 6(6) (2009) 1047-1058.
60. L.S. Tan, J.N. Mohd, K. Mohd, Acidic and basic dyes removal by adsorption on chemically treated mangrove barks, *Int. J. Appl. Sci. Technol.* 2(3) (2012) 270-276.

61. B. Meroufel, O. Benali, M. Benyahia, Y. Benmoussa, M.A. Zenasni, Adsorptive removal of anionic dye from aqueous solutions by Algerian kaolin: Characteristics, isotherm, kinetic and thermodynamic studies, *J. Mater. Environ. Sci.* 4 (2013) 482-491.
62. M.-H. Baek, C.O. Ijagbemi, O. Se-Jin, D.-S. Kim, Removal of malachite green from aqueous solution using degreased coffee bean, *J. Hazard. Mater.* 176 (2010) 820-828. DOI: [10.1016/j.jhazmat.2009.11.110](https://doi.org/10.1016/j.jhazmat.2009.11.110)
63. L. Ćurković, D. Asperger, S. Babic, J. Zupan, Adsorption of enrofloxacin onto natural zeolite: Kinetics, thermodynamics, isotherms and error analysis, *Indian Journal of Chemical Technology* 25 (2018) 565-571.
64. P. Ramachandran, R. Vairamuthu, S. Ponnusamy, Adsorption isotherms, kinetics, thermodynamics and desorption studies of reactive orange16 on activated carbon derived from ananas comosus carbon, *J. Eng. Appl. Sci.* 11 (2011) 15-26.
65. R. Ramadoss, D. Subramaniam, Adsorption of chromium using blue green algae-modeling and application of various isotherms, *Int. J. Chem. Technol.* 10 (2018) 1-22. DOI: [10.3923/ijct.2018.1.22](https://doi.org/10.3923/ijct.2018.1.22)
66. A.S. Ozcan, B. Erdem, A. Ozcan, Adsorption of Acid Blue 193 from aqueous solutions onto Na-bentonite and DTMA-bentonite, *J. Colloid Interface Sci.* 280(1) (2004) 44-54. DOI: [10.1016/j.jcis.2004.07.035](https://doi.org/10.1016/j.jcis.2004.07.035)
67. J. Kamau, G. Kamau, Modeling of experimental adsorption isotherm data for chlorothalonil by Nairobi river sediment, *Mod. Chem. Appl.* 5 (2017) 203. doi: [10.4172/2329-6798.1000203](https://doi.org/10.4172/2329-6798.1000203)
68. H.K. Boparai, M. Joseph, D.M. O'Carroll, Kinetics and thermodynamics of cadmium ion removal by adsorption onto nano zerovalent iron particles, *J. Hazard. Mater.* 186 (2011) 458–465. <https://doi.org/10.1016/j.jhazmat.2010.11.029>
69. M.I. Temkin, V. Pyzhev, Kinetics of ammonia synthesis on promoted iron catalyst, *Acta USSR* 12 (1940) 327–356.
70. N. Ayawei, A.T. Ekubo, D. Wankasi, E.D. Dikio, Adsorption of congo red by Ni/Al-CO₃: equilibrium, thermodynamic and kinetic studies, *Oriental Journal of Chemistry* 31 (2015) 1307–1318. DOI: <http://dx.doi.org/10.13005/ojc/310307>
71. T.V.N. Padmesh, K. Vijayaraghavan, G. Sekaran, M. Velan, Application of two and three-parameter isotherm models; biosorption of Acid Red 88 onto *Azolla microphylla*. *Bioremediation J.* 10 (2006) 37. <https://doi.org/10.1080/10889860600842746>
72. S. Ahmadi, C.A. Igwegbe, S. Rahdar, Z. Asadi, The survey of application of the linear and nonlinear kinetic models for the adsorption of nickel (II) by modified multi-walled carbon nanotubes, *Appl. Water Sci.* 9 (2019) 98. <https://doi.org/10.1007/s13201-019-0978-9>
73. K. Mohanty, D. Das, M.N. Biswas, Adsorption of phenol from aqueous solutions using activated carbons prepared from *Tectona grandis* sawdust by ZnCl₂ activation, *Chem. Eng. J.* 115 (2005) 121–131. <https://doi.org/10.1016/j.cej.2005.09.016>
74. M.C. Menkiti, A.O. Okoani, M.I. Ejimofor, Adsorptive study of coagulation treatment of paint wastewater using novel *Brachystegia eurycoma* extract, *Appl. Water Sci.* 8 (2018) 189. <https://doi.org/10.1007/s13201-018-0836-1>
75. A. Jawad, D. Al-Heetim, R. Abd Rashid, Biochar from orange (*Citrus sinensis*) peels by acid activation for methylene blue adsorption, *Iranian Journal of Chemistry and Chemical Engineering* 38(2) (2019) 91-105.

76. M. Mesbah, S. Hamedshahraki, S. Ahmadi, M. Sharifi, C.A. Igwegbe, Hydrothermal synthesis of LaFeO₃ nanoparticles adsorbent: Characterization and application of error functions for adsorption of fluoride, *MethodsX* 7 (2020) 100786. <https://doi.org/10.1016/j.mex.2020.100786>
77. S. Rahdar, A. Rahdar, C.A. Igwegbe, F. Moghaddam, S. Ahmadi, Synthesis and physical characterization of nickel oxide nanoparticles and its application study in the removal of ciprofloxacin from contaminated water by adsorption: Equilibrium and kinetic studies, *Desal. Water Treat.* 141 (2019) 386–393. DOI: [10.5004/dwt.2019.23473](https://doi.org/10.5004/dwt.2019.23473)
78. T.N. Ramesh, D.V. Kirana, A. Ashwini, T.R. Manasa, Calcium hydroxide as low cost adsorbent for the effective removal of indigo carmine dye in water, *Journal of Saudi Chemical Society* 21(2) (2017) 165-171. <https://doi.org/10.1016/j.jscs.2015.03.001>
79. N. Ouslimani, M.Z.M. Bouregghda, Removal of direct dyes from wastewater by cotton fiber waste, *Int. J. Waste Resour.* 8 (2018) 330. DOI: [10.4172/2252-5211.1000330](https://doi.org/10.4172/2252-5211.1000330)
80. C.A. Igwegbe, P.C. Onyechi, O.D. Onukwuli, Kinetic, isotherm and thermodynamic modelling on the adsorptive removal of malachite green on *Dacryodes edulis* seeds, *J. Sci. Eng. Res.* 2 (2015) 23-39.
81. C.A. Igwegbe, P.C. Onyechi, O.D. Onukwuli, I.C. Nwokedi, Adsorptive treatment of textile wastewater using activated carbon produced from *Mucuna pruriens* seed shells, *World J. Eng. Technol.* 4 (2016) 21-37. <https://doi.org/10.4236/wjet.2016.41003>
82. P. Sampranpiboon, P. Charnkeitkong, Equilibrium isotherm, thermodynamic and kinetic studies of lead adsorption onto pineapple and paper waste sludges, *International Journal of Energy and Environment* 4(3) (2010).
83. E. Eren, O. Cubuk, H. Ciftci, B. Eren, B. Caglar, Adsorption of basic dye from aqueous solutions by modified sepiolite: Equilibrium, kinetics and thermodynamics study, *Desalination* 252 (2010) 88–96. <https://doi.org/10.1016/j.desal.2009.10.020>
84. R.F.P.M. Moreira, J.L. Soares, H.J. Jose, A.E. Rodrigues, The removal of reactive dyes using high-ash char, *Braz. J. Chem. Eng.* 18 (2001) 327-336. [doi:10.1590/S0104-66322001000300011](https://doi.org/10.1590/S0104-66322001000300011)
85. J.O. Ighalo, A.G. Adeniyi, Mitigation of diclofenac pollution in aqueous media by adsorption, *ChemBioEng. Rev.* 7(2) (2020) 1–15. <https://doi.org/10.1002/cben.201900020>
86. J.O. Ighalo, A.G. Adeniyi, Adsorption of pollutants by plant bark derived adsorbents: An empirical review, *J. Water Process. Eng.* 35 (2020) 101228. <https://doi.org/10.1016/j.jwpe.2020.101228>
87. B. Nagy, C. Mânzatu, A. Măicăneanu, C. Indolean, B.-T. Lucian, C. Majdik, Linear and nonlinear regression analysis for heavy metals removal using *Agaricus bisporus* macrofungus, *Arab. J. Chem.* 10 (2017) S3569–S3579. <https://doi.org/10.1016/j.arabjc.2014.03.004>
88. S. Ahmad, L. Mohammadi, A. Rahdar, S. Rahdar, R. Dehghani, C.A. Igwegbe, G.Z. Kyzas, Acid dye removal from aqueous solution by using neodymium (iii) oxide nanoadsorbents, *Nanomaterials (Basel, Switzerland)* 10(3) (2020) 556. doi: [10.3390/nano10030556](https://doi.org/10.3390/nano10030556)
89. I.A.W. Tan, B.H. Hameed, Removal of crystal violet dye from aqueous solutions using rubber (*Hevea brasillensis*) seed shell-based biosorbent, *Desal. Water Treat.* 48(1-3) (2012) 174–181. [doi:10.1080/19443994.2012.698810](https://doi.org/10.1080/19443994.2012.698810)

(2020) ; <http://www.jmaterenvirosci.com>